# Volatile communication in plants relies on a KAI2-mediated signaling pathway

Shannon Stirling, Angelica Guercio, Ryan Patrick, Xing-Qi Huang, Matthew Bergman, Varun Dwivedi, Ruy Kortbeek, Yi-Kai Liu, Fuai Sun, W. Andy Tao, et al.

# Title: Volatile communication in plants relies on a KAI2-mediated signaling pathway

**Authors:** Shannon A. Stirling[1], Angelica M. Guercio[2], Ryan M. Patrick[1,3], Xing-Qi Huang[3,4], Matthew E. Bergman[3,4], Varun Dwivedi[3,4,†], Ruy W.J. Kortbeek[3,4], Yi-Kai Liu[4], Fuai Sun[2], W. Andy Tao[4,5,6,7], Ying Li[1,3], Benoît Boachon[3,4,8], Nitzan Shabek[2] & Natalia Dudareva[1,3,4,*]

**Affiliations:**

[1] Department of Horticulture and Landscape Architecture, Purdue University, West Lafayette, IN 47907, USA

[2] Department of Plant Biology, College of Biological Sciences, University of California–Davis, Davis, CA, 95616, USA

[3] Purdue Center for Plant Biology, Purdue University, West Lafayette, IN 47907, USA

[4] Department of Biochemistry, Purdue University, 175 South University St., West Lafayette, IN 47907-2063, U.S.A.

[5] Department of Chemistry, Purdue University, West Lafayette, IN, 47907, USA

[6] Department of Medicinal Chemistry and Molecular Pharmacology, Purdue University, West Lafayette, IN, 47907, USA

[7] Purdue Institute for Cancer Research, Purdue University, West Lafayette, IN, 47907, USA

[8] Université Jean Monnet Saint-Etienne, CNRS, LBVpam UMR 5079, F-42023, Saint-Etienne, France

† Present address: Division of Biochemistry, Interdisciplinary Plant Group, University of Missouri, Columbia, Missouri 65211, USA

* Corresponding author. E-mail: dudareva@purdue.edu

**Abstract:** Plants are constantly exposed to volatile organic compounds (VOCs) released during plant-plant communication, within-plant self-signaling and plant-microbe interactions. Therefore, understanding VOC perception and downstream signaling is vital for unraveling the mechanisms behind information exchange in plants, which remain largely unexplored. Using the hormone-like function of volatile terpenoids in reproductive organ development as a system with a visual marker for communication, we demonstrated that a petunia karrikin-insensitive receptor, PhKAI2ia, stereo-specifically perceives the (−)-germacrene D signal, triggering a KAI2-mediated signaling cascade and affecting plant fitness. This study uncovers the role(s) of the intermediate clade of KAI2 receptors, illuminates the involvement of a KAI2ia-dependent signaling pathway in volatile communication and provides new insights into plant olfaction and the long-standing question about the nature of potential endogenous KAI2 ligand(s).

**One-Sentence Summary:** Inter-organ plant communication occurs stereospecifically via volatile terpenoids and a KAI2-mediated signaling pathway.

**Main Text:** Volatile organic compounds (VOCs) are released by all kingdoms of life, including bacteria and fungi, mediating intra- and inter-specific communications above- and below-ground (*1*). Specifically, plant VOCs emitted from vegetative organs into the atmosphere and from roots into the soil play key roles in attracting pollinators and other beneficial organisms, defending plants against herbivores and pathogens, and protecting against abiotic stresses (*2*). In addition, plants are constantly exposed to volatiles as a part of plant-plant and plant-microbe interactions, and within-plant signaling (*3*-*5*). Therefore, perception of volatiles and downstream signaling are essential parts of communication given that receivers must decrypt the chemical language to distinguish signals from background odors and respond to specific VOC cues. Due to the plethora of biological processes dependent on VOCs, significant progress has been made towards understanding the biosynthesis of plant VOCs and their regulation, and, in recent years, the molecular mechanisms involved in VOC emission (*6*-*8*). Yet, little is known about how plants perceive VOCs and trigger cellular response(s) that may enhance their resilience and overall fitness.

In animals, VOCs are recognized by odorant receptors in the olfactory neural system, which constitute the largest G-protein-coupled receptor (GPCR) family (*9*). In contrast, plants have only a few GPCR proteins that appear to have different functions (*10*). To date, only limited information exists about the receptors for airborne signals in plants. These examples include (*i*) ETR and NTHK1 receptors for volatile plant hormone ethylene (*11, 12*), (*ii*) salicylic acid-binding protein-2 (SABP2), a receptor for airborne methyl salicylate (*13*), (*iii*) a KAI2 receptor for volatile karrikins (*14*), small bioactive organic compounds produced by wildfires (*15, 16*), and (*iv*) TOPLESS-like proteins (TPLs), transcriptional co-suppressors with β-caryophyllene-binding activity, which are involved in VOC sensing in tobacco (*17*).

The absence of reliable molecular markers of the perception state in receiving plants greatly slowed the progress in the investigation of plant olfaction. However, we have recently discovered that in *Petunia hybrida* flowers volatile terpenoids can move between different organs via natural fumigation (*3*). Produced by terpene synthase 1 (PhTPS1) in flower tubes and released before anthesis inside the buds, sesquiterpenes accumulate in reproductive organs and are required for normal pistil development. Since the loss of sesquiterpene fumigation by downregulation of *PhTPS1* transcript levels significantly decreases pistil weight and stigma size (*3*), we used this hormone-like function of volatile terpenoids as a visual marker for communication to investigate the molecular mechanisms underlying VOC perception and signaling.

The reduced stigma growth in *PhTPS1*-RNAi (*tps1*) flowers could be a result of a direct effect of VOCs on reproductive organ development or indirect consequences of either increased growth of colonizing bacteria or their products on transgenic pistils (*3*). Therefore, *tps1* pistils were shortly treated with bleach, which, while leaving pistils alive, effectively reduced bacterial levels (fig. S1A), and were grown within wild-type or *tps1* tubes. Independent of treatment, *tps1* pistils grown within *tps1* tubes exhibited a reduced stigma size phenotype relative to those grown within wild-type tubes (fig. S1B), suggesting that the terpenoid signal released from tubes is required for normal pistil development independent of the stigma microbial community.

**VOC impacts stigma size via karrikin-like signaling pathway** To determine the molecular mechanisms underlying inter-organ VOC perception and signaling, we generated RNA sequencing (RNA-seq) data sets from wild-type and *tps1* stigmas on day -1 and day +1 postanthesis. Only minor differences were observed on day -1 postanthesis in transgenics versus wild-type, while comparative analysis of transcript abundances on day +1 showed ~four-fold

increase in the number of differentially expressed genes (fig. S2A). Gene Ontology (GO) enrichment analysis revealed that eight out of 23 GO terms (~35%) enriched among downregulated genes were associated with multiple stress responses including those to ethylene and its upstream regulator karrikin (*18*) (fig. S2B). Therefore, we hypothesized that a karrikin-like signaling pathway is involved in VOC-mediated communication.

Karrikins are not endogenously produced by plants but are bioactive compounds of smoke, which stimulate the gemination of seeds across over 1,200 plant species from more than 80 genera (*15, 16*). They also regulate numerous plant developmental processes unrelated to fires including ethylene-dependent root growth (*18*) in addition to their important roles in biotic and abiotic responses (*19*). Karrikins are perceived by the karrikin insensitive2 (KAI2) receptor (*14, 20*), for which most angiosperms have one or more copies of the encoding gene(s). The widespread occurrence of genes for karrikin responses in plant species from non-fire-prone environments, their evolutionary conservation among the angiosperms and the origin of KAI2-like proteins prior to land plant evolution (as they already exist in charophytes) (*21-23*) implies that the core function of the karrikin signaling pathways is to sense endogenous KAI2 ligand(s), the nature of which is yet unknown (*14, 15, 20*).

GO term analysis identified eight genes belonging to "response to karrikin" (GO:0080167) that were downregulated in the *tps1* mutant relative to the wild-type in our RNA-seq datasets (fig. S3A). In contrast, the expression of petunia homologues of known karrikin signaling pathway genes remained largely unchanged with the exception of *KAI2ia* (fig. S3B). Using identified differentially expressed genes as markers of volatile signal response, we analyzed their transcript levels by quantitative real-time polymerase chain reaction (qRT-PCR) in wild-type and *tps1* stigmas grown within different volatile conditions. All eight genes were strongly downregulated upon VOC depletion in *tps1* and wild-type pistils grown within *tps1* tubes relative to wild-type pistil/wild-type tube control (fig. S4A). Moreover, complementation of *tps1* stigmas via fumigation with volatiles emitted by wild-type tubes (*3*) restored, to a different extent, expression of karrikin-responsive genes, implying that VOC and karrikin signaling may share similar molecular mechanisms.

**PhKAI2ia is required for VOC perception and response** Unlike most angiosperms, the *KAI2* genes in the Lamiids, which comprise ~15% of all flowering plants including Solanales (*24*), form three subclades: conserved (*KAI2c*), intermediate (*KAI2i*) and divergent (*KAI2d*) (*25-27*). Like other members of Solanaceae family, the petunia genome contains four *KAI2* genes, two of which belong to the conserved (*PhKAI2c*) and two to the intermediate (*PhKAI2i*) clades (fig. S5). Out of the four *KAI2* genes, *PhKAI2ia* expression was the highest in stigma based on qRT-PCR analysis (Fig. 1A) and dependent on VOC levels. It was upregulated in the reduced VOC environment within *tps1* tubes (Fig. 1B and fig. S4B) highlighting its likely role in sensing volatiles. Therefore, to investigate whether VOC signaling pathway relies on the KAI2ia receptor, we generated "deaf" receivers by RNAi downregulation of *PhKAI2ia* under control of cauliflower mosaic virus 35S promoter. Three independent homozygous lines with 57-70% reduced *PhKAI2ia* transcript levels (Fig. 1C) displayed smaller stigma size phenotype (Fig. 1D and E) similar to that in *tps1* transgenic plants (Fig. 1E). However, unlike *tps1* flowers (*3*), the terpenoid emission from tubes of *PhKAI2ia*-RNAi flowers were not statistically different from that of wild-type and empty vector control (fig. S6). In addition, *PhKAI2ia* tubes were able to sustain normal growth of wild-type stigma and recover the reduced size of *tps1*, but not *kai2ia*, stigmas (Fig. 1F, right panel). Moreover, the small *PhKAI2ia* pistil phenotype was independent of tube VOC production (Fig. 1F) and *PhKAI2ia*-RNAi downregulation did not affect expression

of other *PhKAI2* genes, *PhKAI2ca, PhKAI2cb and PhKAI2ib*, in transgenic *PhKAI2ia* pistils (fig. S7). Taken together, these results provide genetic evidence for the involvement of PhKAI2ia in the perception of volatile signal(s). They also show that other *PhKAI2* genes, which exhibit varying tissue-specific expression profiles (fig. S8) and encode proteins with 74 to 84% amino acid identity to PhKAI2ia (fig. S5), are unable to compensate for the reduced PhKAI2ia activity likely due to different ligand binding specificity. Similar to *tps1* flowers which lack terpene fumigation (*3*), the inability of transgenic *PhKAI2ia*-RNAi plants to perceive the volatile signal affected seed production by reducing the number of seeds by 23 to 47 % per flower without impact on the individual seed weight (Fig. 1G), indicating the decreased fitness in the absence of normal volatile perception.

**PhKAI2ia stereo-specifically perceives (−)-germacrene D** To determine whether the reproductive organ growth-promoting effect is a unique property of (*i*) (−)-germacrene D, the major product of PhTPS1 (fig. S9), (*ii*) volatile sesquiterpenes or volatile monoterpenes as classes of compounds, or (*iii*) volatiles in general, gas phase complementation assays were performed. Wild-type stigmas were grown in the presence of (−)- and (+)-germacrene D, as these two enantiomers are known to possess different bioactivities (*28, 29*), sesquiterpenes cadinene, the most abundant VOC detected in petunia pistils (*3*), caryophyllene, farnesol, and nerolidol, monoterpene linalool and phenylpropene eugenol. Karrikins ($KAR_1$ and $KAR_2$) were also included in these fumigation experiments to determine whether, after being taken in by pistils (fig. S10), these compounds influence petunia stigma growth. Out of the tested compounds, only (−)-germacrene D was able to promote normal growth of wild-type pistils (Fig. 2A and B) and restore normal stigma size phenotype in *tps1* (Fig. 2C), but not in "deaf" *kai2ia* (Fig. 2D), pistils. Moreover, expression analysis of petunia karrikin-responsive genes in reconstructed flowers with wild-type pistils fumigated with (−)- and (+)-germacrene D revealed that only the (−)-enantiomer was able to sustain mRNA at levels similar to pistils grown within wild-type tubes (fig. S11A). Exceptions included the *PhSTS* gene which was upregulated in response to (−)-germacrene D, and *PhCRR55* and *PhO04544* genes, the mRNA levels of which were only partially restored. Similar to treatment with tubes from different genotypes (Fig. 1B), *PhKAI2ia* gene expression in pistils was sensitive to the presence of airborne (−)-germacrene D around the pistil, with expression being the highest in the absence of this sesquiterpene (fig. S11B). In contrast to *PhKAI2ia*, expression of *PhKAI2ib*, *PhKAI2ca* and *PhKAI2cb* remained unaffected by fumigation treatments suggesting that other petunia KAI2 receptors are insensitive to the (−)-germacrene D (fig. S11B).

To biochemically analyze and directly test for ligand affinity, displacement hydrolysis assays with Yoshimulactone Green (YLG), differential scanning fluorimetry (DSF) and limited proteolysis-mass spectrometry (LiP-MS) (fig. S12) (*30*), were performed with purified recombinant PhKAI2ia and PhKAI2ca (fig. S13) in the presence of (−)- and (+)-germacrene D. PhKAI2ca was chosen for these experiments as a representative of the conserved clade (fig. S5) and its encoding gene exhibits in the stigma the second highest expression out of four petunia *PhKAI2s* (Fig. 1A). Notably, PhKAI2ia hydrolysis activity was impacted by a wide range of concentrations of (−)-germacrene D and only by high non-physiological concentrations of the (+)-enantiomer (Fig. 3A). PhKAI2ca hydrolysis activity was comparatively low and not impacted by either (−)- or (+)-germacrene D. The calculated $IC_{50}$ = 158 µM (measured as normalized percentages of fluorescein product release) shows a (−)-germacrene D dose dependent inhibition response of PhKAI2ia and is in the range of the (−)-germacrene D concentration (> 60 µM) estimated based on its pool size in petunia stigmas (*3*). Interestingly,

GR24, a synthetic strigolactone analog, also inhibited YLG hydrolysis by both PhKAI2 receptors (fig. S14).

DSF showed no thermal shift of either PhKAI2ia or PhKAI2ca in the presence of (−)- and (+)-germacrene D, possibly due to known limitations of this technique with volatile ligands (*27*, *31*, *32*) (fig. S15), thus we used LiP-MS, another widely used method to identify protein-small molecule interactions and validated it by using AtKAI2 with one of its known ligands, (−)-GR24 (fig. S16). LiP-MS identified 300 peptides for both PhKAI2s covering the entirety of each protein. Only PhKAI2ia exhibited conformational changes when treated with (−)-germacrene D, resulting in significant increases in the intensities of 5 peptides compared to either PhKAI2ia treatment with the (+)-germacrene D or PhKAI2ca samples treated with (−)- or (+)-germacrene D (Fig. 3B). Modeling of the PhKAI2ia structure by AlphaFold2 (*33*) (fig. S17A) followed by molecular dynamics docking with (−)-germacrene D (fig. S17B) revealed a conserved ligand-binding pocket that coordinates the docked (−)-germacrene D within the active site (fig. S17C-E). About 17 amino acids within the pocket including G25, F26, catalytic S95, L96, F124, F134, L142, F157, V161, F174, I193, F194, L218, A219, V220, catalytic H246, and L247 coordinate the interaction with (−)-germacrene D (fig. S17C-F). Several of these residues were previously found to not only coordinate other synthetic ligands like GR24, but also help differentiate ligand sensitivity (*34*-*37*). These structurally altered sequences (shown in boxes) were located near the N-terminal and C-terminal regions of PhKAI2ia and found to coincide with the potential binding sites of (−)-germacrene D determined by the simulation results (fig. S17F).

**PhKAI2ia-mediated VOC signaling requires MAX2 proteins** Sensing a signal is a crucial first step in communication, yet the subsequent downstream transduction events upon perception are equally critical to propagating cellular changes. Studies have shown that MAX2, an F-box protein of the SKP1-CUL1-F-box (SCF) E3 ubiquitin ligase complex, is an essential part of both strigolactone and karrikin signaling (*38-40*), which mediates the ubiquitination and proteasomal degradation of transcriptional repressors (*39*, *41-44*). Like other members of the Lamiids, which contain the unique KAI2i clade, petunia has two copies of *MAX2* genes that are ubiquitously expressed across aerial plant tissues and encode proteins PhMAX2a and PhMAX2b with 81% amino acid identity (fig. S18). To investigate whether PhKAI2ia-mediated VOC signaling shares common molecular mechanisms with the strigolactone and karrikin pathways and acts via MAX2 protein(s), subcellular localization of potential interactors was analyzed. Fluorescently tagged fusion proteins, PhKAI2ia and PhKAI2ca, when transiently expressed in Arabidopsis protoplasts (fig. S19) and *Nicotiana benthamiana* leaves (fig. S20) showed dual localization in the nucleus and cytoplasm similar to their Arabidopsis homologues (*45*). As predicted (*39*), PhMAX2a showed localization primarily to the nucleus, while PhMAX2b demonstrated dual localization, in the nucleus and cytoplasm, when expressed in protoplasts (fig. S19). Taken together, these results suggest that PhKAI2ia and PhKAI2ca co-occur with PhMAX2a and PhMAX2b in the nucleus allowing potential interactions. In addition, the co-occurrence of PhMAX2b with PhKAI2ia and PhKAI2ca in the cytoplasm suggests a previously unexplored role of a MAX2 in this compartment.

To determine whether PhKAI2ia forms a complex with PhMAX2a/b and the role of (−)-germacrene D in these interactions, pull-down experiments in vitro and in vivo were performed with tagged PhKAI2ia, PhKAI2ca and PhMAX2a/b in the presence of (−)- and (+)-germacrene D. Our in vitro results with recombinant PhMAX2a produced in baculovirus-insect cells (fig. S21) show that (*i*) PhKAI2ia interacts with PhMAX2a in the presence of (−)- but not (+)-germacrene D (Fig. 4A) and (*ii*) this interaction is specific for PhKAI2ia and does not occur with

PhKAI2ca (Fig. 4B). Additionally, (−)-germacrene D facilitates in vivo complex formation between PhKAI2ia and PhMAX2a as well as PhMAX2b (Fig. 4C), while no interactions were detected when *PhKAI2ca* was transiently overexpressed in petunia stigmas instead of *PhKAI2ia* (Fig 4D).

**(−)-Germacrene D promotes degradation of transcriptional co-repressor SMAX1** It is well established that karrikins induce degradation of known signaling repressor SUPPRESSOR OF MAX2 1 (SMAX1) upon interaction with KAI2 receptor which leads to activation of downstream signaling cascade (*46-48*). To test whether SMAX1 degradation is involved in (−)-germacrene D mediated PhKAI2ia signaling, the degradation of both PhSMAX1a and PhSMAX1b was analyzed upon transient expression in stigmas of different petunia backgrounds: wild-type, *tps1* mutants ("mute emitters") and *kai2ia* transgenics ("deaf receivers") of their D2 domains previously shown to be sufficient in strigolactone and karrikin signaling (fig. S22) (*44, 46, 49*). The deficiency in (−)-germacrene D signal, either due to a compromised perception in *kai2ia* stigmas or inability to produce signal in *tps1* tubes, resulted in no PhSMAX1a degradation in contrast to 51% decrease in PhSMAX1a levels in wild-type stigmas which were naturally fumigated by volatiles produced in flower tubes (Fig. 4E and F). No volatile-dependent degradation of PhSMAX1b was found in the analyzed petunia backgrounds (fig. S23), suggesting that unlike PhSMAX1a, PhSMAX1b is not involved in (−)-germacrene D signaling.

**Conclusions.** Using the hormone-like function of volatile terpenoids in petunia reproductive organ development as a system with a visual marker for communication, this study provides strong evidence that (*i*) perception of volatiles is compound-specific and affects plant fitness; (*ii*) out of four *PhKAI2* genes, only expression of *PhKAI2ia* negatively correlates with the levels of emitted terpenoids; (*iii*) PhKAI2ia, a karrikin-insensitive receptor of a unique intermediate clade stereo-specifically recognizes (−)-germacrene D; (*iv*) (−)-germacrene D-mediated communication relies on the KAI2ia-dependent signaling pathway and shares some transcriptional gene targets with the karrikin responses, and (*v*) the KAI2ia-dependent (−)-germacrene signal transduction operates via PhMAX2 ubiquitin ligase degradation of PhSMAX1a and other PhKAI2 receptors are unable to compensate for reduced PhKAI2ia activity (Fig. 5). While (−)-germacrene D represents a potential karrikin-like ligand and can bind PhKAI2ia receptor, mediates formation of PhKAI2ia-PhMAX2a/b complex and facilitates signal transduction via PhSMAX1a degradation, it does not contain a butenolide moiety shared by karrikins and strigolactones (*15, 16, 50*). Since gas complementation and pulldown assays were performed in vivo, it is possible that (−)-germacrene D is metabolized by endogenous enzymes in planta to a more potent ligand for PhKAI2ia receptor, which requires further investigation. Many plants produce germacrene, however, its production in the majority of species is dominated by (−)-germacrene D (*51*). Interestingly, in addition to the existence of a specific plant receptor for (−)-germacrene D described here, heliothine moths possess neurones with high sensitivity and selectivity to (−)-germacrene D (*28, 52*). It highlights the importance of this compound not only for within plant communication but also in a broader ecological context for plant-insect interaction.

## References and Notes


1. A. C. Vlot, M. Rosenkranz, Volatile compounds—The language of all kingdoms? *Journal of Experimental Botany* **73**, 445-448 (2022).
2. H. Bouwmeester, R. C. Schuurink, P. M. Bleeker, F. Schiestl, The role of volatiles in plant communication. *The Plant Journal* **100**, 892-907 (2019).

3. B. Boachon *et al.*, Natural fumigation as a mechanism for volatile transport between flower organs. *Nature Chemical Biology* **15**, 583-588 (2019).
4. J. Midzi *et al.*, Stress-induced volatile emissions and signalling in inter-plant communication. *Plants* **11**, 2566 (2022).
5. A. Russo, S. Pollastri, M. Ruocco, M. M. Monti, F. Loreto, Volatile organic compounds in the interaction between plants and beneficial microorganisms. *Journal of Plant Interactions* **17**, 840-852 (2022).
6. F. Adebesin *et al.*, Emission of volatile organic compounds from petunia flowers is facilitated by an ABC transporter. *Science* **356**, 1386-1388 (2017).
7. P. Liao *et al.*, Cuticle thickness affects dynamics of volatile emission from petunia flowers. *Nature Chemical Biology* **17**, 138-145 (2021).
8. P. Liao *et al.*, Emission of floral volatiles is facilitated by cell-wall non-specific lipid transfer proteins. *Nature Communications* **14**, 330 (2023).
9. Y. Jiang, H. Matsunami, Mammalian odorant receptors: Functional evolution and variation. *Current Opinion in Neurobiology* **34**, 54-60 (2015).
10. D. Urano, A. M. Jones, Heterotrimeric G protein–coupled signaling in plants. *Annual Review of Plant Biology* **65**, 365-384 (2014).
11. C. Xie *et al.*, Serine/threonine kinase activity in the putative histidine kinase-like ethylene receptor NTHK1 from tobacco. *The Plant Journal* **33**, 385-393 (2003).
12. R. F. Lacey, B. M. Binder, How plants sense ethylene gas — The ethylene receptors. *Journal of Inorganic Biochemistry* **133**, 58-62 (2014).
13. Q. Gong *et al.*, Molecular basis of methyl-salicylate-mediated plant airborne defence. *Nature* **622**, 139-148 (2023).
14. M. T. Waters *et al.*, Specialisation within the DWARF14 protein family confers distinct responses to karrikins and strigolactones in Arabidopsis. *Development* **139**, 1285-1295 (2012).
15. D. C. Nelson, G. R. Flematti, E. L. Ghisalberti, K. W. Dixon, S. M. Smith, Regulation of seed germination and seedling growth by chemical signals from burning vegetation. *Annual Review of Plant Biology* **63**, 107-130 (2012).
16. G. R. Flematti, E. L. Ghisalberti, K. W. Dixon, R. D. Trengove, A compound from smoke that promotes seed germination. *Science* **305**, 977-977 (2004).
17. A. Nagashima *et al.*, Transcriptional regulators involved in responses to volatile organic compounds in plants. *Journal of Biological Chemistry* **294**, 2256-2266 (2019).
18. S. M. Swarbreck, Phytohormones interplay: Karrikin signalling promotes ethylene synthesis to modulate roots. *Trends in Plant Science* **26**, 308-311 (2021).
19. M. T. Waters, D. C. Nelson, Karrikin perception and signalling. *New Phytologist* **237**, 1525-1541 (2023).
20. G. R. Flematti, K. W. Dixon, S. M. Smith, What are karrikins and how were they ‘discovered’ by plants? *BMC Biology* **13**, 108 (2015).
21. R. Bythell-Douglas *et al.*, Evolution of strigolactone receptors by gradual neo-functionalization of KAI2 paralogues. *BMC Biology* **15**, 52 (2017).
22. C. H. Walker, K. Siu-Ting, A. Taylor, M. J. O’Connell, T. Bennett, Strigolactone synthesis is ancestral in land plants, but canonical strigolactone signalling is a flowering plant innovation. *BMC Biology* **17**, 70 (2019).
23. P.-M. Delaux *et al.*, Origin of strigolactones in the green lineage. *New Phytologist* **195**, 857-871 (2012).
24. N. F. Refulio-Rodriguez, R. G. Olmstead, Phylogeny of Lamiidae. *American Journal of Botany* **101**, 287-299 (2014).

25. C. E. Conn *et al.*, Convergent evolution of strigolactone perception enabled host detection in parasitic plants. *Science* **349**, 540-543 (2015).
26. G. Xiong, J. Li, Steven M. Smith, Evolution of strigolactone perception by seeds of parasitic plants: Reinventing the wheel. *Molecular Plant* **9**, 493-495 (2016).
27. Y. K. Sun *et al.*, Divergent receptor proteins confer responses to different karrikins in two ephemeral weeds. *Nature Communications* **11**, 1264 (2020).
28. M. Stranden, A. K. Borg-Karlson, H. Mustaparta, Receptor neuron discrimination of the germacrene D enantiomers in the moth *Helicoverpa armigera*. *Chemical Senses* **27**, 143-152 (2002).
29. I. Prosser *et al.*, Enantiospecific (+)- and (−)-germacrene D synthases, cloned from goldenrod, reveal a functionally active variant of the universal isoprenoid-biosynthesis aspartate-rich motif. *Archives of Biochemistry and Biophysics* **432**, 136-144 (2004).
30. S. Schopper *et al.*, Measuring protein structural changes on a proteome-wide scale using limited proteolysis-coupled mass spectrometry. *Nature Protocols* **12**, 2391-2410 (2017).
31. M. T. Waters *et al.*, A Selaginella moellendorffii Ortholog of KARRIKIN INSENSITIVE2 Functions in Arabidopsis Development but Cannot Mediate Responses to Karrikins or Strigolactones. *The Plant Cell* **27**, 1925-1944 (2015).
32. J. Yao *et al.*, An allelic series at the KARRIKIN INSENSITIVE 2 locus of Arabidopsis thaliana decouples ligand hydrolysis and receptor degradation from downstream signalling. *The Plant Journal* **96**, 75-89 (2018).
33. M. Mirdita *et al.*, ColabFold: Making protein folding accessible to all. *Nature Methods* **19**, 679-682 (2022).
34. S. Carbonnel *et al.*, *Lotus japonicus* karrikin receptors display divergent ligand-binding specificities and organ-dependent redundancy. *PLOS Genetics* **16**, e1009249 (2021).
35. A. M. Guercio *et al.*, Structural and functional analyses explain Pea KAI2 receptor diversity and reveal stereoselective catalysis during signal perception. *Communications Biology* **5**, 126 (2022).
36. A. M. Guercio, M. Palayam, N. Shabek, Strigolactones: Diversity, perception, and hydrolysis. *Phytochemistry Reviews* **22**, 339-359 (2023).
37. S. E. Martinez *et al.*, A KARRIKIN INSENSITIVE2 paralog in lettuce mediates highly sensitive germination responses to karrikinolide. *Plant Physiology* **190**, 1440-1456 (2022).
38. D. C. Nelson *et al.*, F-box protein MAX2 has dual roles in karrikin and strigolactone signaling in *Arabidopsis thaliana*. *Proceedings of the National Academy of Sciences* **108**, 8897-8902 (2011).
39. P. Stirnberg, I. J. Furner, H. M. Ottoline Leyser, MAX2 participates in an SCF complex which acts locally at the node to suppress shoot branching. *The Plant Journal* **50**, 80-94 (2007).
40. M. T. Waters, C. Gutjahr, T. Bennett, D. C. Nelson, Strigolactone signaling and evolution. *Annual Review of Plant Biology* **68**, 291-322 (2017).
41. L. Jiang *et al.*, DWARF 53 acts as a repressor of strigolactone signalling in rice. *Nature* **504**, 401-405 (2013).
42. J. P. Stanga, S. M. Smith, W. R. Briggs, D. C. Nelson, SUPPRESSOR OF MORE AXILLARY GROWTH2 1 controls seed germination and seedling development in Arabidopsis *Plant Physiology* **163**, 318-330 (2013).
43. I. Soundappan *et al.*, SMAX1-LIKE/D53 family members enable distinct MAX2-dependent responses to strigolactones and karrikins in Arabidopsis. *The Plant Cell* **27**, 3143-3159 (2015).

44. N. Shabek *et al.*, Structural plasticity of D3–D14 ubiquitin ligase in strigolactone signalling. *Nature* **563**, 652-656 (2018).
45. X.-D. Sun, M. Ni, HYPOSENSITIVE TO LIGHT, an alpha/beta fold protein, acts downstream of ELONGATED HYPOCOTYL 5 to regulate seedling de-etiolation. *Molecular Plant* **4**, 116-126 (2011).
46. A. Khosla *et al.*, Structure–function analysis of SMAX1 reveals domains that mediate its karrikin-induced proteolysis and interaction with the receptor KAI2. *The Plant Cell* **32**, 2639-2659 (2020).
47. J. Zheng *et al.*, Karrikin signaling acts parallel to and additively with strigolactone signaling to regulate rice mesocotyl elongation in darkness. *The Plant Cell* **32**, 2780-2805 (2020).
48. Y.-J. Park, J. Y. Kim, C.-M. Park, SMAX1 potentiates phytochrome B-mediated hypocotyl thermomorphogenesis. *The Plant Cell* **34**, 2671-2687 (2022).
49. L. Tal *et al.*, C-terminal conformational changes in SCF-D3/MAX2 ubiquitin ligase are required for KAI2-mediated signaling. *New Phytologist* **239**, 2067-2075 (2023).
50. A. de Saint Germain *et al.*, An histidine covalent receptor and butenolide complex mediates strigolactone perception. *Nature Chemical Biology* **12**, 787-794 (2016).
51. N. Bülow, W. A. König, The role of germacrene D as a precursor in sesquiterpene biosynthesis: Investigations of acid catalyzed, photochemically and thermally induced rearrangements. *Phytochemistry* **55**, 141-168 (2000).
52. M. Stranden *et al.*, (–)-Germacrene D receptor neurones in three species of heliothine moths: structure-activity relationships. *Journal of Comparative Physiology A* **189**, 563-577 (2003).
53. A. Bombarely *et al.*, Insight into the evolution of the Solanaceae from the parental genomes of *Petunia hybrida*. *Nature Plants* **2**, 16074 (2016).
54. R. M. Patrick, X.-Q. Huang, N. Dudareva, Y. Li, Dynamic histone acetylation in floral volatile synthesis and emission in petunia flowers. *Journal of Experimental Botany* **72**, 3704-3722 (2021).
55. D. Risso, K. Schwartz, G. Sherlock, S. Dudoit, GC-content normalization for RNA-seq data. *BMC Bioinformatics* **12**, 480 (2011).
56. S.-D. Yoo, Y.-H. Cho, J. Sheen, Arabidopsis mesophyll protoplasts: A versatile cell system for transient gene expression analysis. *Nature Protocols* **2**, 1565-1572 (2007).
57. X.-Q. Huang, R. Li, J. Fu, N. Dudareva, A peroxisomal heterodimeric enzyme is involved in benzaldehyde synthesis in plants. *Nature Communications* **13**, 1352 (2022).
58. G. Wu, D. H. Robertson, C. L. Brooks III, M. Vieth, Detailed analysis of grid-based molecular docking: A case study of CDOCKER—A CHARMm-based MD docking algorithm. *Journal of Computational Chemistry* **24**, 1549-1562 (2003).
59. S. Jo, T. Kim, V. G. Iyer, W. Im, CHARMM-GUI: A web-based graphical user interface for CHARMM. *Journal of Computational Chemistry* **29**, 1859-1865 (2008).
60. J. C. Phillips *et al.*, Scalable molecular dynamics on CPU and GPU architectures with NAMD. *The Journal of Chemical Physics* **153**, 044130 (2020).

## Acknowledgments

**Funding:** This work was supported by a grant from the National Science Foundation IOS-2139804 to N.D. and N.S., by the USDA National Institute of Food and Agriculture Hatch Projects number 177845 and 1013620 to N.D. and Y.L., respectively, by the USDA National

Institute of Food and Agriculture Postdoctoral grant 2019-67012-29660 to R.M.P., and NIH grant 3RF1AG064250 to W.A.T. The authors thank Dr. Joseph H. Lynch for isolation of two RNA samples for RNA-seq.

**Author contributions:** N.D. and N.S. conceived the project. S.A.S. generated transgenic plants and performed RNA analysis and complementation assays. A.M.G. performed displacement assays and analyzed protein-protein interactions in vitro. F.S. produced recombinant proteins in insect cells. R.M.P., B.B., M.E.B., and Y.L. generated and analyzed RNA-seq datasets. B.B. analyzed stereochemistry of germacrene D. X.-Q.H. and V.D. performed subcellular localization. X.-Q.H. and S.A.S. performed phylogenetic analysis. X.-Q.H. and A.M.G. performed modeling. V.D. and R.W.J.K. analyzed protein-protein interactions in planta. Y.K.L. and W.A.T. performed LiP-MS analysis. N.D. and M.E.B. wrote the manuscript with contributions from all authors. All authors read and edited the manuscript.

**Competing interests:** The authors declare no competing interests.

**Data and materials availability:** All data are available in the main text or supplementary materials. The generated RNA-seq datasets were deposited in the NCBI Gene Expression Omnibus under GEO accession GSE245080, and the sequences reported in this paper have been deposited in GenBank database as OR700010-OR700017. *Petunia axillaris* genomic data were obtained from http://solgenomics.net using *Petunia axillaris* v1.6.2 genome database (*53*). All peptide mass spectrometry data were deposited to the ProteomeXchange Consortium via the jPOST partner repository as PXD048893.

## Figure Legends

**Fig. 1. *PhKAI2ia* is required for sesquiterpene perception and response in petunia stigmas.** Expression in stigmas of *PhKAI2s* (**A**), Ph*KAI2ia* within reconstituted flowers of pistil/tube (p/t) genotype combinations (**B**) and Ph*KAI2ia* in wild-type (WT), empty vector control (EV), and *PhKAI2ia*-RNAi lines (**C**). (**A-C)** *P*-values were determined by two-way ANOVA and Dunnett's multiple comparisons test. In (**C**) *P*-values are relative to WT (black) and EV (blue). *tps1*, *PhTPS1*-RNAi. (**D**) Cross sections of representative stigmas on day 1 postanthesis. Scale bars, 300 μm. (**E**) Stigma major axis length in WT, *tps1*, EV, and *PhKAI2ia*-RNAi lines on day 1 postanthesis normalized to WT. (**F**) Stigma major axis length of WT, *tps1*, and *PhKAI2ia*-RNAi line 18 (*kai2ia*) pistils grown in tubes of WT (left), *tps1* (middle), and *kai2ia* (right) normalized to WT pistils in WT tubes. (**E** and **F**) *P*-values were determined by two-way ANOVA with Dunnett's multiple comparisons test relative to WT (black) and *tps1* (blue) stigmas within each panel. (**G**) Seed production in *PhKAI2ia-RNAi* lines. *P*-values were determined by one-way ANOVA with Tukey multiple comparison test relative to WT. Data are means ± SD (**A-C**, n = 3 biological replicates; **E**, n = 10-12; **F**, n = 10; **G**, n = 4).

**Fig. 2. Pistil growth phenotype response is specific to (−)-germacrene D.** Stigma major axis length of wild-type (WT) (**A** and **B**), *PhTPS1*-RNAi (*tps1*) (**C**), and *PhKAI2ia*-RNAi (line 18) (**D**) pistils grown in WT and *tps1* tubes as well as in the presence of volatiles shown at the bottom. Results are presented relative to WT pistil growth within WT tubes (**A** and **B**) and *tps1* pistil growth in WT tubes (**C** and **D**) set as 100%. All data are means ± SD (**A**, n = 35-47 biological replicates; **B**, n = 15; **C**, 29-41; **D**, n = 15). *P*-values were determined by two-way ANOVA with Dunnett's multiple comparisons test relative to the WT (black) and *tps1* (blue)

tubes in **A**-**C** and relative to the *tps1* (black) and *PhKAI2ia*-RNAi (line 18) (blue) pistils grown in the WT tubes in **D**. KAR1 and KAR2, karrikins 1 and 2, respectively. Hexane was used as a solvent control.

**Fig. 3. PhKAI2ia binds specifically to (−)-germacrene D.** (**A**) Kinetics of YLG hydrolysis by PhKAI2ia and PhKAI2ca in the presence of (+)- and (−)-germacrene D. Colored lines represent non-linear regression curve fit with datapoints for triplicates shown in dots (Supplementary Data 2). The inhibitory dose-response curve for (−)-germacrene D is shown on the right. One-way ANOVA and Tukey test were used to determine significant differences between runs with different germacrene D concentrations. Only PhKAI2ia samples with (−)-germacrene D showed significant differences relative to 0 µM control with *P*-values at (−)-germacrene D concentrations: 125 µM, $P \leq 0.05$; 250 µM, $P \leq 0.0001$; 500 µM, $P \leq 0.0001$; 1 mM, $P \leq 0.0001$. All other comparisons showed no significant differences except when 1 mM (+)-germacrene D was added to PhKAI2ia ($P \leq 0.05$). (**B**) Conformational changes in PhKAI2ia and PhKAI2ca upon incubation with (+)- and (−)-germacrene D determined by LiP-MS and visualized by volcano plots. Each point represents a peptide. For each protein and condition, a total of 303 peptides were identified, which provided 100% protein coverage. Peptides passing the significance cutoff ($|\log_2(\text{Difference})| > 1$, q-value < 0.05, as determined by Student's *t*-test and a permutation test) are colored in red.

**Fig. 4. (−)-Germacrene D is required for PhKAI2ia-PhMAX2 complex formation and PhSMAX1 degradation.** In vitro GST pulldown of GST-PhKAI2ia and His-MBP-PhMAX2a (**A**) and GST-PhKAI2ia, GST-PhKAI2ca, and His-MBP-PhMAX2a (**B**) in the presence or absence of (+)- or (−)-germacrene D. In vivo complex formation shown by HA pulldown of HA-PhKAI2ia (**C**) and HA-PhKAI2ca (**D**) with PhMAX2a-FLAG, PhMAX2b-FLAG, or YFP from wild-type petunia stigmas transiently expressing respective proteins and grown in the presence of (+)- or (−)-germacrene D. YFP was used as a negative control for the specificity of PhKAI2 interactions. (**E**) HA-pulldown of HA-PhSMAX1a from wild-type, *tps1* and *kai2ia* (line 18) petunia stigmas transiently expressing HA-PhSMAX1a and GFP as expression control and grown in tubes of the same genetic background. Actin is shown as a loading control. Proteins were visualized via Western blots with anti-His and anti-GST (**A** and **B**), anti-HA and anti-FLAG (**C** and **D**), and anti-HA antibodies and anti-GFP (**E**) antibodies as indicated. (**F**) Quantification of PhSMAX1a degradation in different genetic backgrounds. The level of HA-PhSMAX1a was normalized to co-expressed GFP and presented as means ± SD (n = 4 biological replicates including one in **E**). *P*-values were determined by a two-tailed paired *t*-test relative to WT.

**Fig. 5. Proposed model for (−)-germacrene D KAI2ia–dependent signaling in petunia pistils.** Under normal wild-type growth conditions, KAI2ia perceives (−)-germacrene D, which leads to the recruitment of MAX2a/b and subsequent targeting of SMAX1a for degradation, resulting in normal pistil development and seed yield. Under *tps1* RNAi knockdown conditions, the decreased (−)-germacrene D signal (“mute emitters”) reduces KAI2ia-MAX2a/b complex formation and SMAX1a degradation, resulting in smaller pistils and lower seed yield relative to wild-type plants. Under *kai2ia* RNAi knockdown conditions, less complex formation occurs due to the diminished ability to perceive (−)-germacrene D signal (“deaf receivers”), resulting in similar pistil and seed phenotypes as in “mute emitters”.

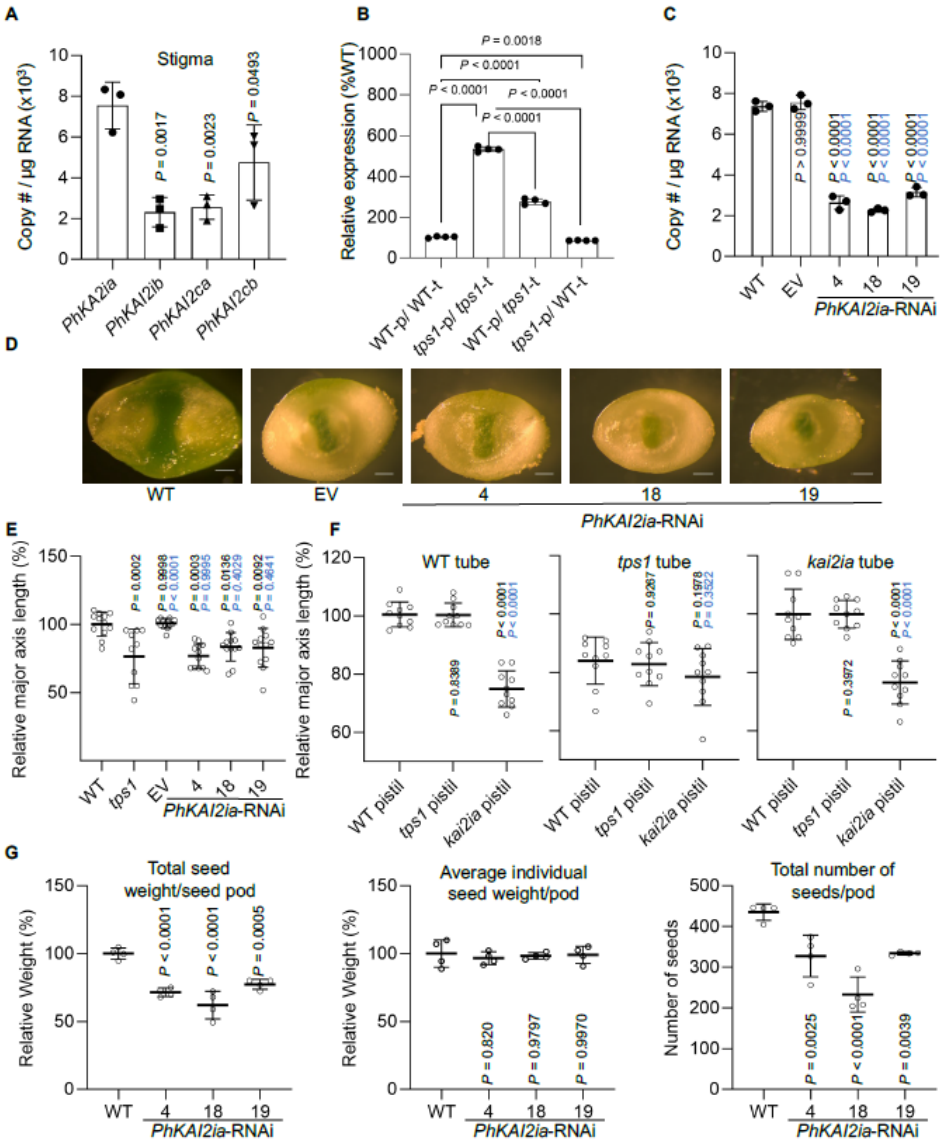


**Fig. 1. *PhKAI2ia* is required for sesquiterpene perception and response in petunia stigmas.** Expression in stigmas of *PhKAI2s* (**A**), Ph*KAI2ia* within reconstituted flowers of pistil/tube (p/t) genotype combinations (**B**) and Ph*KAI2ia* in wild-type (WT), empty vector control (EV), and *PhKAI2ia*-RNAi lines (**C**). (**A-C)** *P*-values were determined by two-way ANOVA and Dunnett's multiple comparisons test. In (**C**) *P*-values are relative to WT (black) and EV (blue). *tps1*, *PhTPS1*-RNAi. (**D**) Cross sections of representative stigmas on day 1 postanthesis. Scale bars, 300 µm. (**E**) Stigma major axis length in WT, *tps1*, EV, and *PhKAI2ia*-RNAi lines on day 1 postanthesis normalized to WT. (**F**) Stigma major axis length of WT, *tps1*, and *PhKAI2ia*-RNAi line 18 (*kai2ia*) pistils grown in tubes of WT (left), *tps1* (middle), and *kai2ia* (right) normalized to WT pistils in WT tubes. (**E** and **F**) *P*-values were determined by two-way ANOVA with Dunnett's multiple comparisons test relative to WT (black) and *tps1* (blue) stigmas within each panel. (**G**) Seed production in *PhKAI2ia-RNAi* lines. *P*-values were determined by one-way ANOVA with Tukey multiple comparison test relative to WT. Data are means ± SD (**A-C**, n = 3 biological replicates; **E**, n = 10-12; **F**, n = 10; **G**, n = 4).

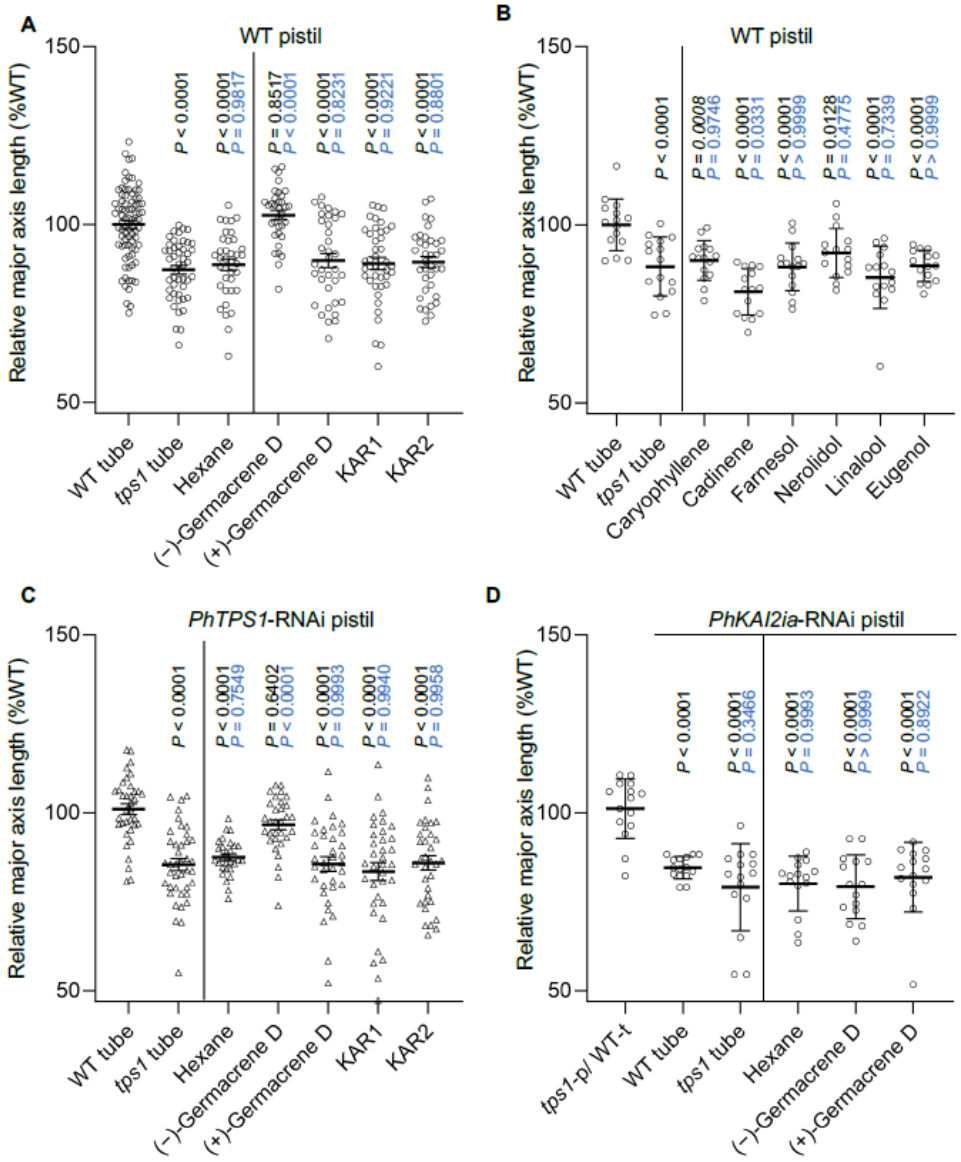


**Fig. 2. Pistil growth phenotype response is specific to (−)-germacrene D.** Stigma major axis length of wild-type (WT) (**A** and **B**), *PhTPS1*-RNAi (*tps1*) (**C**), and *PhKAI2ia*-RNAi (line 18) (**D**) pistils grown in WT and *tps1* tubes as well as in the presence of volatiles shown at the bottom. Results are presented relative to WT pistil growth within WT tubes (**A** and **B**) and *tps1* pistil growth in WT tubes (**C** and **D**) set as 100%. All data are means ± SD (**A**, n = 35-47 biological replicates; **B**, n = 15; **C**, 29-41; **D**, n = 15). *P*-values were determined by two-way ANOVA with Dunnett's multiple comparisons test relative to the WT (black) and *tps1* (blue) tubes in **A**-**C** and relative to the *tps1* (black) and *PhKAI2ia*-RNAi (line 18) (blue) pistils grown in the WT tubes in **D**. KAR1 and KAR2, karrikins 1 and 2, respectively. Hexane was used as a solvent control.

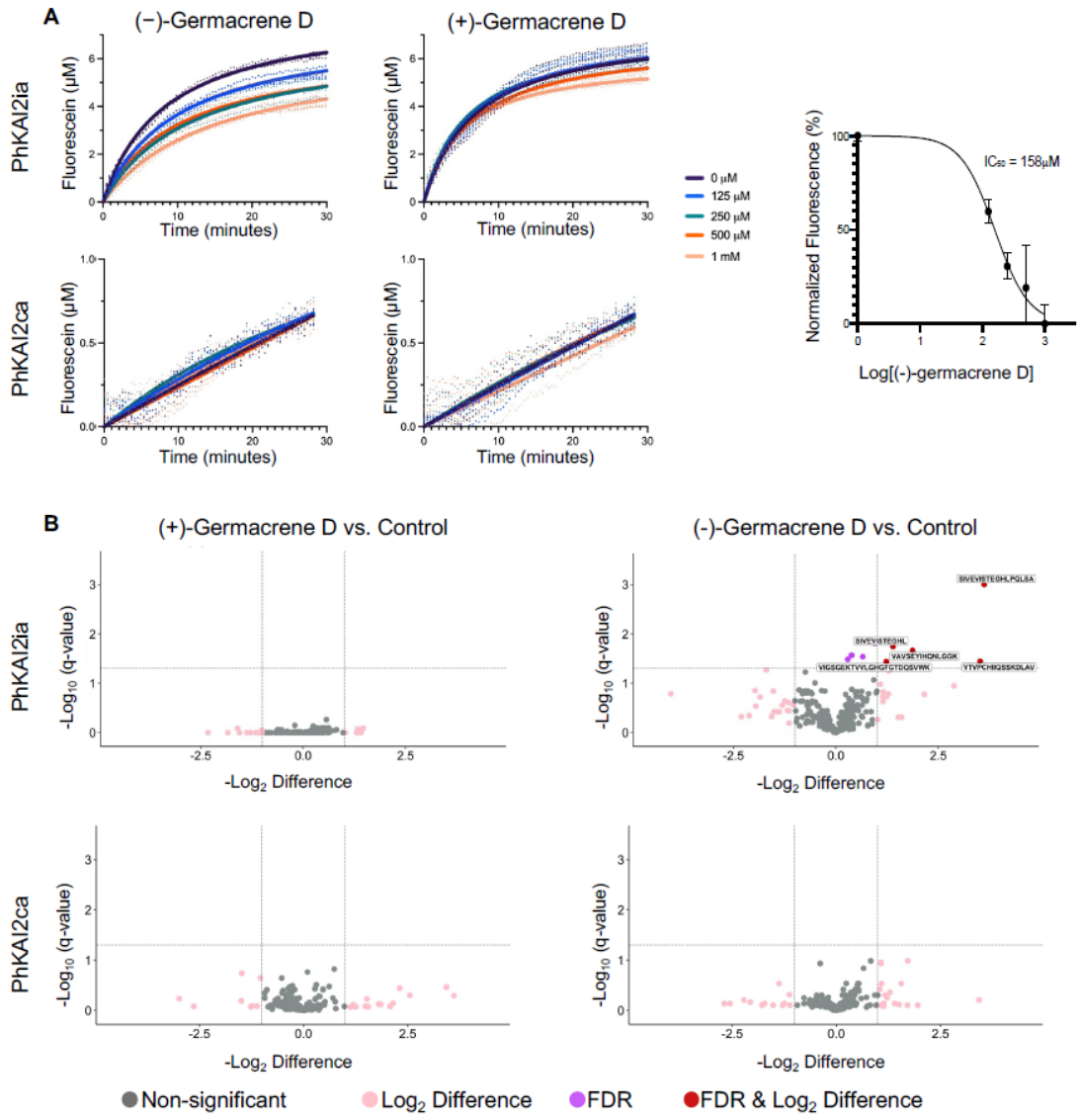


**Fig. 3. PhKAI2ia binds specifically to (−)-germacrene D.** (**A**) Kinetics of YLG hydrolysis by PhKAI2ia and PhKAI2ca in the presence of (+)- and (−)-germacrene D. Colored lines represent non-linear regression curve fit with datapoints for triplicates shown in dots (Supplementary Data 2). The inhibitory dose-response curve for (−)-germacrene D is shown on the right. One-way ANOVA and Tukey test were used to determine significant differences between runs with different germacrene D concentrations. Only PhKAI2ia samples with (−)-germacrene D showed significant differences relative to 0 μM control with *P*-values at (−)-germacrene D concentrations: 125 μM, $P \leq 0.05$; 250 μM, $P \leq 0.0001$; 500 μM, $P \leq 0.0001$; 1 mM, $P \leq 0.0001$. All other comparisons showed no significant differences except when 1 mM (+)-germacrene D was added to PhKAI2ia ($P \leq 0.05$). (**B**) Conformational changes in PhKAI2ia and PhKAI2ca upon incubation with (+)- and (−)-germacrene D determined by LiP-MS and visualized by volcano plots. Each point represents a peptide. For each protein and condition, a total of 303 peptides were identified, which provided 100% protein coverage. Peptides passing the significance cutoff ($|\log_2(\text{Difference})| > 1$, q-value < 0.05, as determined by Student's *t*-test and a permutation test) are colored in red.

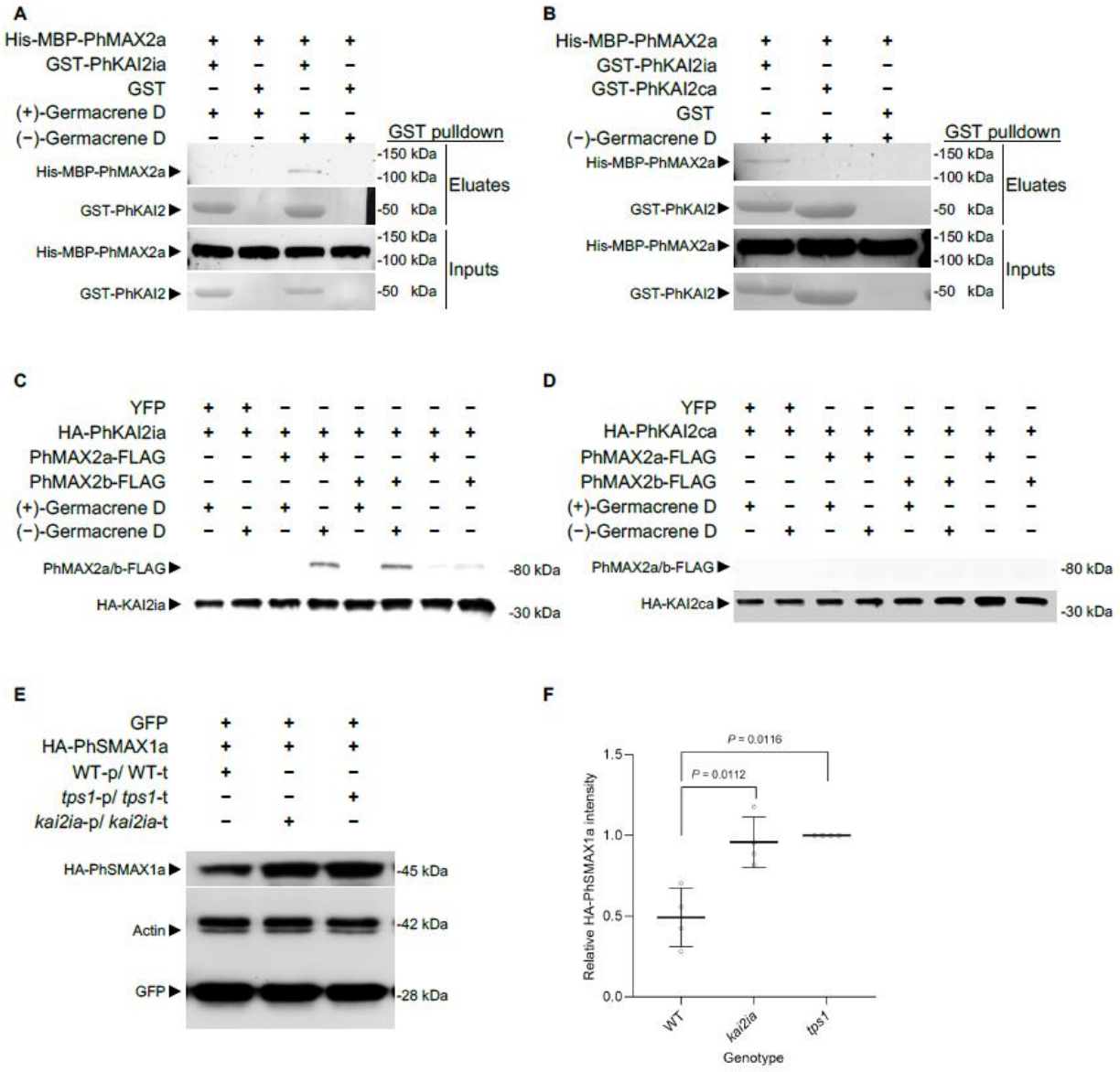


**Fig. 4. (−)-Germacrene D is required for PhKAI2ia-PhMAX2 complex formation and PhSMAX1 degradation.** In vitro GST pulldown of GST-PhKAI2ia and His-MBP-PhMAX2a (**A**) and GST-PhKAI2ia, GST-PhKAI2ca, and His-MBP-PhMAX2a (**B**) in the presence or absence of (+)- or (−)-germacrene D. In vivo complex formation shown by HA pulldown of HA-PhKAI2ia (**C**) and HA-PhKAI2ca (**D**) with PhMAX2a-FLAG, PhMAX2b-FLAG, or YFP from wild-type petunia stigmas transiently expressing respective proteins and grown in the presence of (+)- or (−)-germacrene D. YFP was used as a negative control for the specificity of PhKAI2 interactions. (**E**) HA-pulldown of HA-PhSMAX1a from wild-type, *tps1* and *kai2ia* (line 18) petunia stigmas transiently expressing HA-PhSMAX1a and GFP as expression control and grown in tubes of the same genetic background. Actin is shown as a loading control. Proteins were visualized via Western blots with anti-His and anti-GST (**A** and **B**), anti-HA and anti-FLAG (**C** and **D**), and anti-HA antibodies and anti-GFP (**E**) antibodies as indicated. (**F**) Quantification of PhSMAX1a degradation in different genetic backgrounds. The level of HA-PhSMAX1a was normalized to co-expressed GFP and presented as means ± SD (n = 4 biological replicates including one in **E**). *P*-values were determined by a two-tailed paired *t*-test relative to WT.

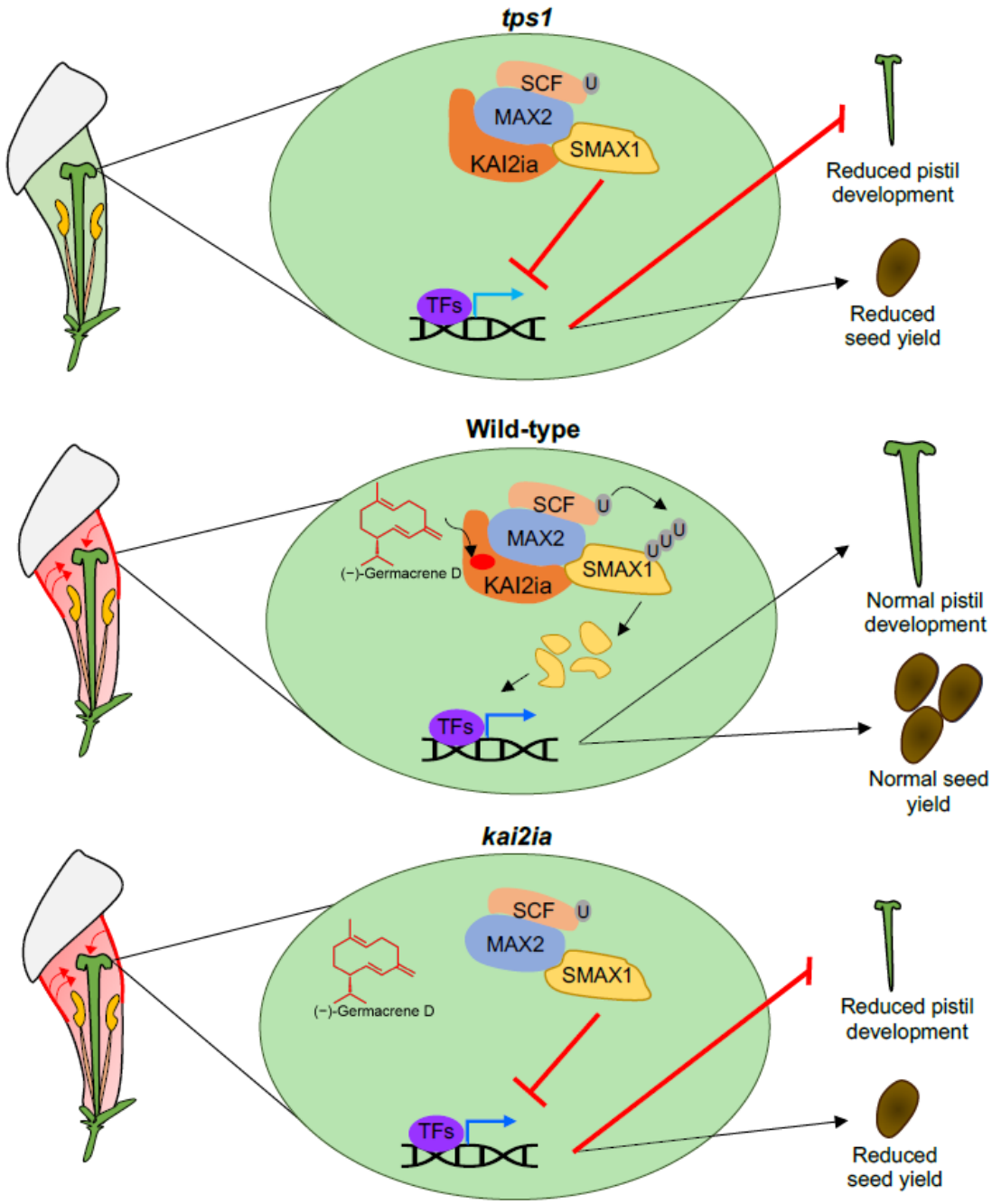


**Fig. 5. Proposed model for (−)-germacrene D KAI2ia–dependent signaling in petunia pistils.** Under normal wild-type growth conditions, KAI2ia perceives (−)-germacrene D, which leads to the recruitment of MAX2a/b and subsequent targeting of SMAX1a for degradation, resulting in normal pistil development and seed yield. Under *tps1* RNAi knockdown conditions, the decreased (−)-germacrene D signal ("mute emitters") reduces KAI2ia-MAX2a/b complex formation and SMAX1a degradation, resulting in smaller pistils and lower seed yield relative to wild-type plants. Under *kai2ia* RNAi knockdown conditions, less complex formation occurs due to the diminished ability to perceive (−)-germacrene D signal ("deaf receivers"), resulting in similar pistil and seed phenotypes as in "mute emitters".